Rare Metal Materials and Engineering
Volume 51, Issue 4, April 2022
Available online at www.rmme.ac.cn

Science Press

Cite this article as: Lu Boxin, Yang Fang, Zhou Yang, et al. Preparation of Powder Metallurgy Titanium Alloy with Bimodal Structure of High Mechanical Properties[J]. Rare Metal Materials and Engineering, 2022, 51(04): 1152-1157.

ARTICLE

Preparation of Powder Metallurgy Titanium Alloy with Bimodal Structure of High Mechanical Properties

Lu Boxin[1], Yang Fang[1,2,3], Zhou Yang[1], Chen Cunguang[1,2,3], Sui Yanli[1,2,3], Guo Zhimeng[1,2,3]

[1] Institute for Advanced Materials and Technology, University of Science and Technology Beijing, Beijing 100083, China; [2] Shunde Graduate School of University of Science and Technology Beijing, Foshan 528399, China; [3] Innovation Group of Marine Engineering Materials and Corrosion Control, Southern Marine Science and Engineering Guangdong Laboratory (Zhuhai), Zhuhai 519000, China

Abstract: Powder metallurgy (PM) Ti6Al4V alloy with a relative density of 99% was prepared by low temperature vacuum sintering using fine Ti6Al4V powder. To eliminate porosity and control the microstructure morphology, forging was performed. The results show that microstructure of as-forged samples is bimodal structure with long lath primary α and $\alpha+\beta$ lamellae. The as-forged samples show tensile properties with ultimate tensile strength (UTS) of 1176 MPa, yield strength (YS) of 1100 MPa, elongation (EL) of 18.2%, and good low-cycle fatigue life. The as-forged PM Ti6Al4V has good fatigue performance with more than 10^5 cycles under the stress of 700 MPa. In order to explore the reasons for good fatigue properties, in-situ observation tests were carried out. It is found that the long lath primary α structure can effectively prevent the crack propagation in the steady propagation stage and prolong the fatigue life. Besides, fully dense structure decreases the fatigue crack initiation. Thus, the bimodal structure shows excellently comprehensive mechanical properties.

Key words: powder metallurgy; Ti6Al4V; bimodal structure; low-cycle fatigue; in-situ observation

Titanium (Ti) alloys have been used in many fields such as aerospace, chemical industry, energy, ship, automobile and medical treatment due to their high strength, low density and excellent corrosion resistance[1-3]. However, because of high manufacturing cost of titanium alloy parts, their application scope is limited[4]. Traditional titanium alloy production processes require remelting and cogging, resulting in cost increase. Powder metallurgy (PM) is considered to be an excellent low-cost process due to its ability to avoid solid-liquid phase transitions and achieve near-net-shape, thereby reducing energy consumption and improving material utilization[5,6]. However, the mechanical properties of PM Ti alloy are generally lower than those of conventional methods, especially in terms of fatigue properties.

The fatigue properties of PM Ti alloy are mainly influenced by both porosity and microstructure. Titanium has a high affinity with interstitial oxygen. When the oxygen content exceeds the critical value of 0.33wt%, the plasticity decreases sharply[7]. For the purpose of reducing the oxygen content, coarse powder or spherical powder is usually used as the raw material. The driving force of coarse powder or spherical powder is low, so the relative density of PM titanium alloy after vacuum sintering is generally 95%~97%[8,9]. The pores can be the initiation point of crack, resulting in low plasticity and fatigue life. In order to increase the density, PM Ti alloy are usually sintered at 1300~1400 °C, far beyond the β-transus temperature. After sintering, coarse original β grains will be obtained. The coarse microstructure caused by high temperature sintering is another reason for poor fatigue properties. In general, the microstructure is basket or Widmanstatten structure consisting of coarse lamellar structure. Some studies[10] have shown that coarse lamellar structure forming the α colony can hinder fatigue crack propagation, but the damage to tensile properties is great.

In addition to high temperature sintering, hot isostatic pressing (HIP) and thermomechanical deformation (TMD) are

Received date: September 18, 2021
Foundation item: National Natural Science Foundation of China (52004027, U21A200305); Scientific and Technological Innovation Foundation of Foshan, USTB (BK21BE001); Fundamental Research Funds for the Central Universities (FRF-GF-20-05A); Innovation Group Project of Southern Marine Science and Engineering Guangdong Laboratory (Zhuhai) (311021013); State Key Lab of Advanced Metals and Materials (2020-Z17)
Corresponding author: Yang Fang, Ph. D., Associate Professor, Institute for Advanced Materials and Technology, University of Science and Technology Beijing, Beijing 100083, P. R. China, Tel: 0086-10-62334376, E-mail: yangfang@ustb.edu.cn

also effective means to promote densification. At present, HIP is one of the most effective densification methods for PM Ti alloy[11,12]. However, HIP cannot optimize the microstructure. Due to the limitation of steel capsule, spherical raw powders and size, HIP is expensive to produce parts. This will weaken the cost advantage of PM Ti alloy. TMD processing is another technique for densification, which is usually carried out by forging, extrusion or rolling[13-15]. Compared with HIP, TMD processing is simple and low-cost. After TMD processing, coarse grains can be broken and refined by recrystallization. Titanium alloy with equiaxed and bimodal microstructure can be obtained by deformation at different temperatures. Fine and near spherical equiaxed structure generally has good strength and plasticity. However, the fatigue strength is low due to poor crack propagation resistance of equiaxed structure[16]. The bimodal structure is obtained by forging at 15~25 °C below β-transus temperature. The bimodal structure has the characteristics of equiaxed structure and lamellar structure at the same time. Some studies have shown that the bimodal structure have excellent comprehensive mechanical properties[17].

In this work, high mechanical property Ti6Al4V alloy was prepared by PM processes. Through forging deformation, densification and microstructure optimization were realized, and the bimodal structure with good comprehensive mechanical properties was obtained. The excellent fatigue property was interpreted by in-situ observing fatigue crack propagation. This investigation is significant in improving the PM Ti alloy.

1 Experiment

Hydrogenation-dehydrogenation (HDH) Ti6Al4V alloy powder was purchased from Tiantailong (Tianjin) Metal Materials Co., Ltd with an average particle size of 10 μm. The chemical composition of raw materials are shown in Table 1. The morphology of powder is shown in Fig.1a. The powder is irregular with low oxygen content of about 800 μL/L. The powder was loaded into a rubber mold in the argon glove box to avoid the increase of impurities. The mold was pressed by cold isostatic pressing machine. The pressure was 300 MPa for 120 s. The green compacts were sintered at 1100, 1150 and 1200 °C for 2 h under a vacuum of 10^{-3} Pa. The dimensions of as-sintered samples were about 90 mm in diameter and 150 mm in length. The as-sintered samples were forged at 1050 °C

Table 1 Impurity elements composition and relative density of samples

Sample	State	Element content/ μL·L^{-1} O	N	H	Relative density/ %
Ti6Al4V powder	-	790	140	150	-
A	1100 °C sintered	1010	180	30	95.2±0.3
B	1150 °C sintered	1010	170	30	99±0.2
C	1200 °C sintered	1020	180	30	99.5±0.2
D	Sample B forged	1010	180	30	100

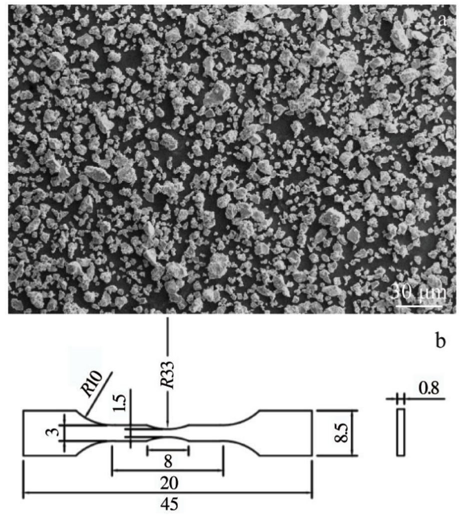

Fig.1 Powder morphology of HDH Ti6Al4V powder (a) and dimensions of in-situ fatigue specimen (b)

into a bar with a diameter of 70 mm and a length of 250 mm. The forged details are as follows. Firstly, the as-sintered bar was heated at 1050 °C for 2 h. The bar was forged repeatedly by an air hammer while rotating the bar to ensure an even reduction in diameter. Subsequently, a hollow round mold with a diameter of 70 mm was used for final forging, and the preheating temperature of the mold was 300 °C. After forging, a bar with a diameter of 70 mm and a length of 250 mm was obtained. Lastly, annealing at 800 °C was carried out to reduce the effect of internal stress.

Densities of as-sintered and as-forged samples were measured by the Archimedes method. All the interstitial O/N/H contents were analysed using Eltra ONH-2000. Because titanium has a high chemical activity, raw powders were put into a nickel capsule in an argon glove box for testing. The block materials were cut into Φ3 mm×3 mm for testing. Each test was measured five times to ensure the data accuracy. Microstructural characterization and fracture were observed using optical microscopy (OM, Axio Imager M2m) and scanning electron microscope (SEM, Philips LEO-1450). The size of α phase was measured from images using Image-Pro. The β-transus temperature of the as-sintered sample was tested by metallographic method. Tensile properties were tested using an electronic universal testing machine (INSTRON-6025). The tensile test was carried out according to ASTM E8 standard at a loading rate of 2 mm/min. In order to observe the fatigue crack propagation, in-situ observation was performed using a specially designed servo-hydraulic fatigue machine (SEM-SERVO, SHIMADZU). This test method has been reported in previous literatures and is an effective method to study the initiation and propagation of fatigue cracks[18,19]. The dimension of the fatigue specimen is shown in Fig. 1b. The fatigue specimen surfaces were ground with 100#~3000# grit emery papers and then polished with diamond abrasive. Finally, the specimens were etched with Kroll's reagent (2vol% HF, 6vol% HNO_3 and 92vol% H_2O). The maximum stress was from 900 MPa to 700 MPa with a decrease of 50 MPa. Besides, the cyclic frequency was 10 Hz and the stress ratio was 0.1.

2 Results and Discussion

2.1 Sintered sample analysis

The impurity content and relative density of as-sintered samples are shown in Table 1. The oxygen content is increased only by about 220 μL/L after sintering. The nitrogen content increases by less than 40 μL/L after sintering, and the hydrogen content decreases due to sintering. Because the contact between powder and air is avoided in the pressing and sintering process, the increase of impurity content is little. With the increase of sintering temperature, the relative density of as-sintered samples increases gradually, as shown in Table 1. When the sample is sintered at 1100 and 1150 °C, the relative density is 95.2% and 99%, respectively. When the sintering temperature is 1200 °C, the relative density is increased to 99.5%. This is mainly caused by the fine powder and low oxygen content. Fine powder increases the contact area between powder particles, and low oxygen content reduces the thickness of oxide film on powder surface, which promotes the formation of sintering neck.

Microstructures of as-sintered samples are observed by optical microscope, as shown in Fig.2. From Fig.2a, it can be seen that the microstructure of sample A (1100 °C) mainly consists of short rod-like α phase and pores. The average length of α phase is about 30 μm and the width is about 16 μm. When the sintering temperature is increased by 50 °C, the pores are less and the α phase grows longer. The length of α phase is about 50 μm and the width is about 16 μm. When the samples are sintered at 1200 °C, there are almost few pores. As shown in Fig. 2c, the microstructure consists of grain boundary α and $\alpha+\beta$ lamellar structure. The original β grain size is about 100 μm. The width of α lamellae and grain boundary α is about 8 and 13 μm, respectively.

Fig. 3 shows the tensile properties of PM Ti6Al4V alloys. The ultimate tensile strength (UTS), yield strength (YS) and elongation (EL) of sample A sintered at 1100 °C are 880 MPa, 800 MPa and 5%, respectively. When the sintering temperature increases to 1150 °C, the UTS, YS and EL further increase to 960 MPa, 890 MPa and 12%, respectively. When the sintering temperature further increases to 1200 °C, the UTS and YS increase to 990 and 920 MPa, while the EL decreases to 8%. The change of tensile properties is caused by pores and microstructure. When the sample is sintered at 1100 and 1150 °C, the increase of UTS, YS and EL is mainly affected by residual pores. Residual pores can become crack source and accelerate crack growth. When the relative density increases from 95% to 99%, with the decrease of pores, the strength and plasticity increase significantly. When the sintering temperature is 1200 °C, the pores are effectively eliminated. The decrease in EL is determined by microstructure. Grain boundary α and $\alpha+\beta$ lamellar structure cause damage to mechanical properties[20]. Through the comparison with other as-sintered samples, as shown in Table 2, it can be seen that the present sample has higher strength and excellent elongation. This result is attributed to high sintering density and short rod-like structure. Therefore, the sample sintered at 1150 °C has good tensile properties and is selected for forging densification to further improve the performance.

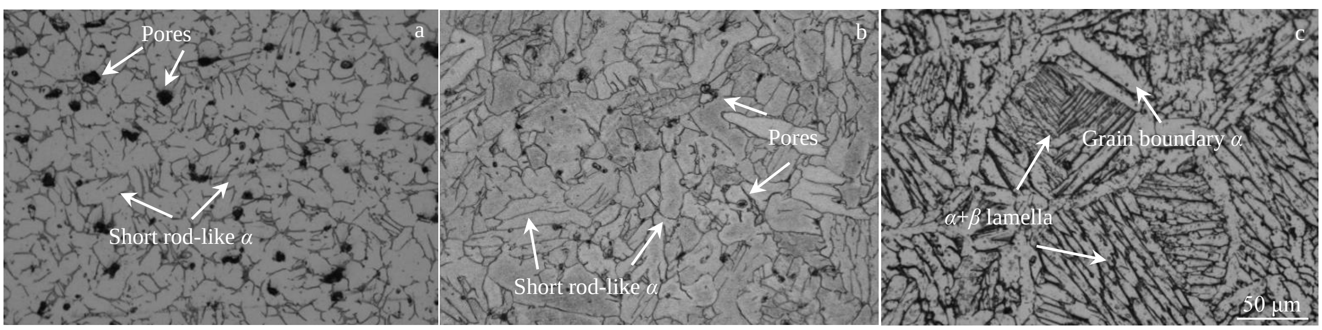

Fig.2 Microstructures of as-sintered Ti6Al4V alloys: (a) sample A, (b) sample B, and (c) sample C

2.2 Forged sample analysis

The β-transus temperature of as-sintered sample is 1000 °C tested by metallographic method. In order to obtain the bimodal structure, forging is carried out at 1050 °C. After forging, the relative density reaches to 100%, as shown in Table 1. And the microstructure is the bimodal structure, as shown in Fig. 4. The microstructure consists of primary α phase and $\alpha+\beta$ lamellae. The shape of primary α phase is long

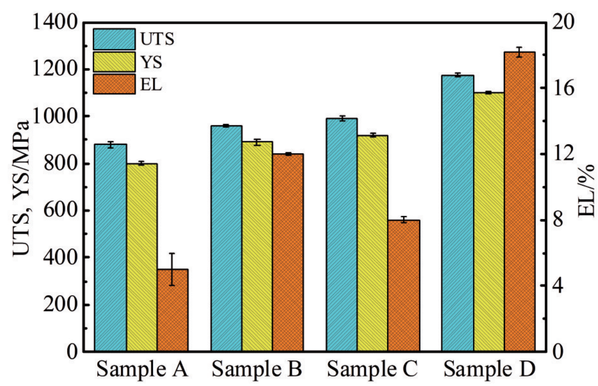

Fig.3 Tensile properties of PM Ti6Al4V alloys

Table 2 Processing, microstructure and average tensile properties of Ti6Al4V alloy

Data source	Processing	Microstructure	UTS/MPa	YS/MPa	EL/%
Present work	As-sintered at 1150 °C	Short rod-like	960	890	12
Present work	PM+forging	Bimodal	1176	1100	18.2
Yan et al[21]	As-sintered	Lamellae	925	848	6
Cao et al[22]	PM+rolling	Lamellae	1250	-	12
Paramore et al[23]	PM+ forging +HT	Bimodal	1093	1004	13
Hu et al[17]	Casting+TMD	Lamellae	900	800	11.8
Peng et al[20]	Casting+TMD+HT	Equiaxed	1100	1030	13

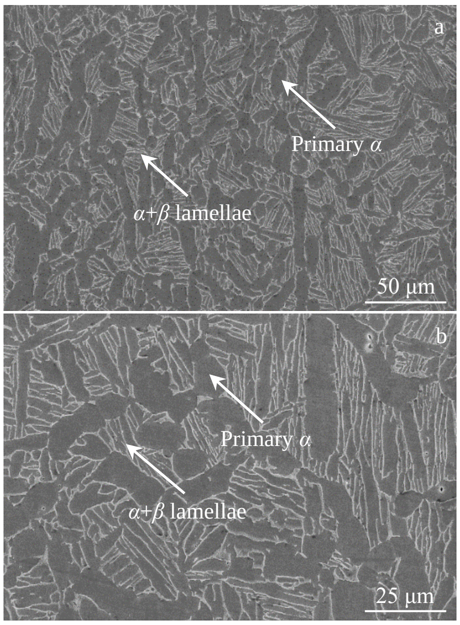

Fig.4 Microstructures of PM Ti6Al4V alloy of sample D under different magnifications: (a) 1000× and (b) 2000×

lath with a length of 30~50 μm and a width of 8~12 μm. The $\alpha+\beta$ lamellae consist of fine secondary α lamellae and intercrystalline β, as shown in Fig.4b. The size of α lamellae is about 1~2 μm in width and 20~30 μm in length.

The tensile properties of as-forged PM Ti6Al4V sample are shown in Fig. 3d. The sample has UTS of 1176 MPa, YS of 1100 MPa and EL of 18.2%. Compared with the as-sintered sample, both the strength (increased by 23.8%) and elongation (increased by 37.9%) are improved. In order to compare the mechanical properties, the properties of Ti6Al4V samples prepared by different processes are listed in Table 2. Compared to traditional PM processes and casting methods, the present method can achieve higher comprehensive mechanical properties.

In order to evaluate the fatigue performance of the as-forged samples, fatigue tests were carried out. The fatigue life curve of sample D is provided in Fig.5. Low cycle fatigue life is significantly increased with decreasing the loading stress. Three experimental samples were tested at each stress value to obtain more reliable results. When the stress is 900 MPa, the sample breaks after 21 065 cycles. As the stress decreases, the number of cycles to fracture increases. When the stress is 700

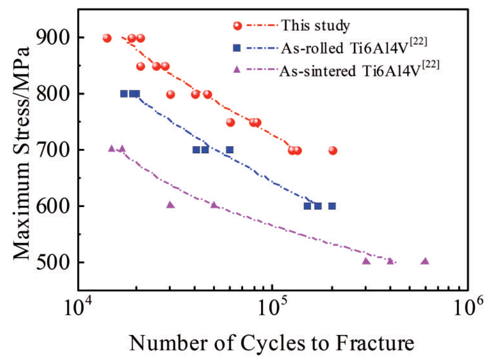

Fig.5 Fatigue life curves of as-forged Ti6Al4V alloy

MPa, the sample breaks after 132 182 cycles. Compared with the reported Ti6Al4V alloy prepared by different methods, as shown in Fig. 5, the as-forged PM Ti alloy in this study has better fatigue performance. In order to explore the reasons for excellent fatigue properties, in-situ fatigue tests were carried out on the samples.

2.3 In-situ fatigue analysis

During the fatigue test, fatigue crack propagation behaviour of the as-forged samples is in-situ observed, as shown in Fig.6. The maximum stress is 750 MPa and the stress ratio is R=0.1. As shown in Fig.6a, with the increase of cycle number, the fatigue crack propagation can be divided into two stages: the stable stage and the accelerated stage[24]. At the first stage, crack propagation is mainly affected by shear stress, as shown in Fig. 6b. A small crack first initiates at the edge of the sample. The crack is 45° to the loading direction. The crack propagates along the interface of primary α and $\alpha+\beta$ lamellae. Then, the crack propagates into the sample in a direction perpendicular to the loading direction, as shown in Fig.6c and 6d. It can be seen that the crack passes through a large number of primary α, and the propagation speed is slow. When the crack grows close to 250 μm, the remaining specimen is not enough to bear the external load, and the crack enters into the accelerated stage, as shown in Fig. 6e and 6f. Finally, the sample fractures after 73 542 cycles.

In the stage of steady propagation, the cracks must pass through or go round each phase to propagate. In such case, the cracks have to propagate at a slow and steady speed. Therefore, the long lath primary α hinders the crack propagation. With the increase in crack propagation, the effect

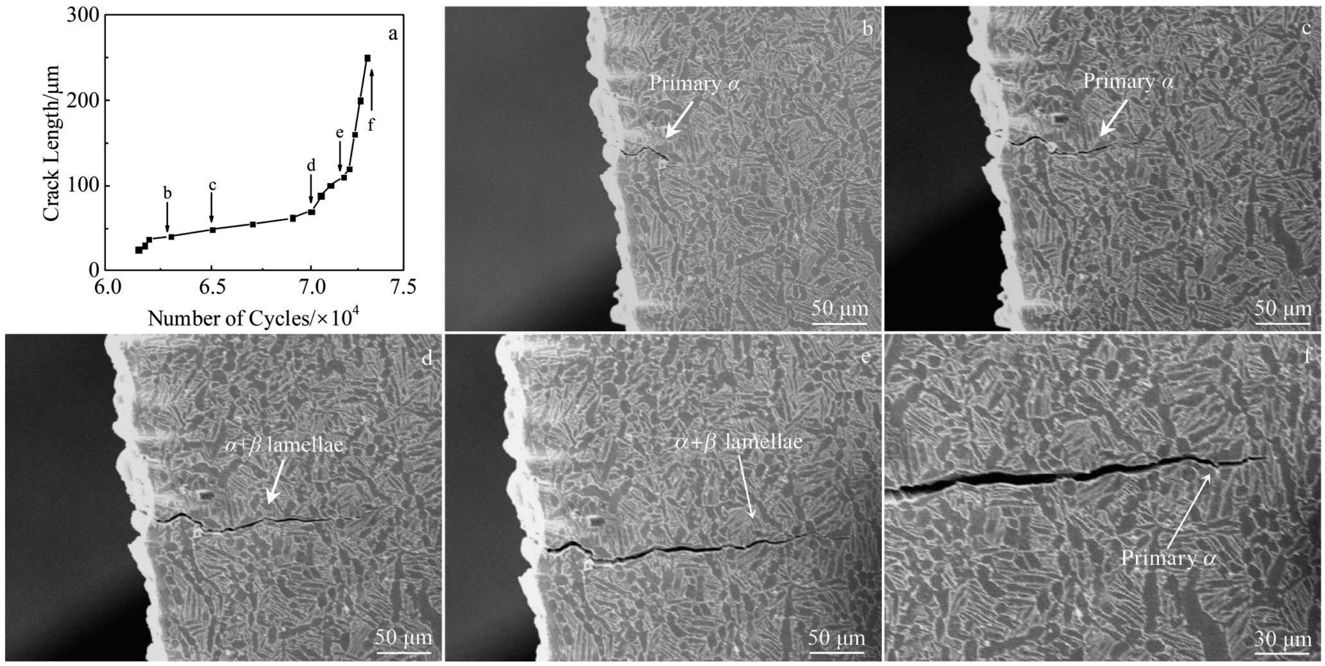

Fig.6 Relation of fatigue crack length with cycle number (a) and SEM images of fatigue crack initiation and propagation behaviour of forged Ti6Al4V alloy after different cycles: (b) 63 000 cycles, (c) 65 000 cycles, (d) 70 500 cycles, (e) 72 000 cycles, and (f) 73 000 cycles

of microstructure on crack propagation becomes weaker, and the crack propagation enters the accelerated propagation stage. As shown in Fig.6a, the stage of steady propagation accounts for most of the time during the crack propagation. Therefore, the long lath primary α microstructure increases the steady propagation stage and prolongs the fatigue life.

Fig.7 shows the fracture morphologies of the in-situ fatigue sample. It can be found that the fatigue crack is initiated on the specimen surface (area A). Some researches have shown that the fatigue crack initiation of PM Ti alloy depends on the sites and size of pores[25]. The decrease of porosity postpones the initiation of fatigue crack and enhances the fatigue performance. In addition, distinct convergent stripes and wide cleavages can be seen from area B. Area B is corresponding to the stable stage, as shown in Fig. 7b. During this stage, the cracks propagate relatively slow. The fatigue fractures are composed of transgranular and intergranular fracture modes. In area C, there are a lot of small ledges and notches, corresponding to the accelerated stage. The main fracture mode is transgranular fracture.

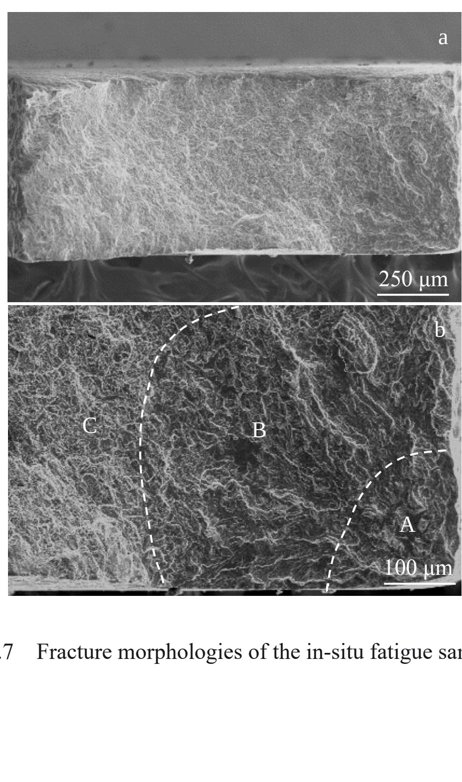

Fig.7 Fracture morphologies of the in-situ fatigue sample

In conclusion, fine structure with few pores avoids the initiation of fatigue cracks. The long lath primary α phase slows down the crack propagation in the steady propagation stage. Under various influencing factors, the fatigue performance of PM Ti alloy increases. Therefore, excellent comprehensive mechanical properties can be obtained by PM combined with forging.

3 Conclusions

1) The as-sintered Ti6Al4V samples with short rod-like structure can be obtained by using fine raw powder and controlling oxygen content of preparing progresses. The as-sintered samples have a relative density of 99%. The microstructure and high density endow good performance with UTS of 960 MPa, YS of 890 MPa and EL of 12%.

2) After forging, the bimodal structure with long lath primary α phase and $\alpha+\beta$ lamellae is obtained and the properties are significantly improved. The tensile properties, including UTS of 1176 MPa, YS of 1100 MPa and EL of 18.2%, are higher than those of traditional PM processes and casting methods.

3) The as-forged PM Ti6Al4V has good fatigue perfor-

mance with more than 10^5 cycles under the stress of 700 MPa. Full dense structure decreases the fatigue crack initiation and long lath primary α phase slows down the crack propagation in the steady propagation stage.

4) Ti6Al4V alloy sintered at low temperature followed by forging to achieve densification has good mechanical and fatigue properties, mainly due to high density and bimodal structure with long lath primary α phase and $\alpha+\beta$ lamellae. This method can be one of the development directions for high-performance PM Ti alloy.

References

1 Montasser M Dewidar, Lim K J. *Journal of Alloys and Compounds*[J], 2008, 454(1): 442

2 Shen J, Chen B, J Umeda *et al*. *Materials Science and Engineering A*[J], 2018, 716(14): 1

3 Liu Ronge, Wang Baoyu, Feng Pengni *et al. Rare Metal Materials and Engineering*[J], 2021, 50(7): 2447 (in Chinese)

4 Froes F H, Friedrich H, Kiese J. *JOM*[J], 2004, 56(11): 40

5 Smeacetto F, Salvo M, Ferraris M. *Surface and Coatings Technology*[J], 2007, 201(24): 9541

6 Wang Haiying, Yang Fang, Lu Boxin *et al*. *Powder Metallurgy*[J], 2021, 64(4): 321

7 Raynova S, Yan C, Fei Y *et al*. *Metallurgical and Materials Transactions A*[J], 2019, 50(11): 4732

8 Bolzoni L, Ruiz-Navas E M, Gordo E. *Materials Characterization*[J], 2013, 84: 48

9 Sidambe A T, Todd I, Hatton P. *Materials Science Forum*[J], 2015, 828-829: 145

10 Guo Ping, Zhao Yongqing, Zeng Weidong *et al*. *Journal of Materials Engineering & Performance*[J], 2015, 24(5): 1865

11 Cai C, Song B, Qiu C *et al*. *Journal of Alloys and Compounds*[J] 2017, 710: 364

12 Alessandro, Abena, Miren. *Advanced Powder Technology*[J], 2019, 30(11): 2451

13 Liang C, Ma M X, Jia M T *et al. Materials Science and Engineering A*[J], 2014, 619(1): 290

14 Dorofeyev V Y, Sviridova A N, Svistun L I. *Russian Journal of Non-Ferrous Metals*[J], 2020, 61(3): 354

15 Zhao Qingyang, Chen Yongnan, Xu Yiku *et al*. *Materials & Design*[J], 2021, 200: 109 457

16 Zhang Xinyu, Mao Xiaonan, Wang Ke *et al*. *Materials Reports*[J], 2021, 35(1): 162 (in Chinese)

17 Hu Zhishou, Shang Guoqiang, Wang Xinnan *et al*. *Journal of Aeronautical Materials*[J], 2020, 40(3): 1

18 Zhang Min, Song Xiping, Yu Long *et al. Materials Science and Engineering A*[J], 2015, 622(12): 30

19 Yu Long, Song Xiping, You Li *et al. Scripta Materialia*[J], 2015, 109: 61

20 Peng Xiaona, Guo Hongzhen, Shi Zhifeng *et al*. *Transactions of Nonferrous Metals Society of China*[J], 2014, 24(3): 682

21 Yan Y, Nash G L, Nash P. *International Journal of Fatigue*[J], 2013, 55: 81

22 Cao Yuankui, Zeng Fanpei, Liu Bin *et al*. *Materials Science and Engineering A*[J], 2016, 654: 418

23 Paramore J D, Fang Z Z, Dunstan M *et al. Scientific Reports*[J], 2017, 7: 41444

24 Romero C, Yang F, Bolzoni L. *International Journal of Fatigue*[J], 2018, 117: 407

25 Xpa B, Sxa B, Gqa B *et al. Materials Science and Engineering A*[J], 2020, 798: 140 110

粉末冶金高性能双态组织钛合金的制备

芦博昕[1]，杨　芳[1,2,3]，周　洋[1]，陈存广[1,2,3]，隋延力[1,2,3]，郭志猛[1,2,3]

(1. 北京科技大学 新材料技术研究院，北京 100083)

(2. 北京科技大学顺德研究生院，广东 佛山 528399)

(3. 南方海洋科学与工程广东实验室(珠海) 海洋工程材料与腐蚀控制创新小组，广东 珠海 519000)

摘　要：采用氢化脱氢粉末，低温真空烧结法制备了相对密度为99%的粉末冶金Ti6Al4V合金。为了消除气孔并控制微观结构形态，对其进行了锻造。结果表明，锻造试样的显微组织为具有长板条初生α和$\alpha+\beta$片层组织的双态结构。锻造后试样可以实现抗拉强度1176 MPa，屈服强度1100 MPa，延伸率18.2%，同时具有良好的低周疲劳寿命。为了探索良好疲劳性能的原因，进行了原位疲劳观察试验。通过对裂纹扩展情况的观察，发现疲劳裂纹扩展可分为2个阶段：稳定阶段和加速阶段。致密组织减少了疲劳源在样品内部的产生。同时双态组织中的的长板条状初生α结构有效地阻止了稳态扩展阶段的疲劳裂纹扩展，从而延长了疲劳寿命。因此，双态结构表现出优异的综合力学性能。

关键词：粉末冶金；Ti6Al4V；双态组织；低周疲劳；原位观察

作者简介：芦博昕，男，1989年生，博士生，北京科技大学新材料技术研究院，北京 100083，电话：010-62334376，E-mail：luboxin2008@126.com